

Oxygen levels affect axon guidance and neuronal migration in *Caenorhabditis elegans*

Roger Pocock & Oliver Hobert

Oxygen deprivation can cause severe defects in human brain development, yet the precise cellular and molecular consequences of varying oxygen levels on nervous system development are unknown. We found that hypoxia caused specific axon pathfinding and neuronal migration defects in *C. elegans* that result from the stabilization of the transcription factor HIF-1 (hypoxia-inducible factor 1) in neurons and muscle. Stabilization of HIF-1 through removal of the proteasomal HIF-1 degradatory pathway phenocopies the hypoxia-induced neuronal defects. Hypoxia-mediated defects in nervous system development depended on signaling through the insulin-like receptor DAF-2, which serves to control the level of reactive oxygen species that also affects axon pathfinding. Hypoxia exerted its effect on axon pathfinding, at least in part, through HIF-1-dependent regulation of the Eph receptor VAB-1. HIF-1-mediated upregulation of VAB-1 protected embryos from hypoxia-induced lethality, but increased VAB-1 levels elicited aberrant axon pathfinding. Similar genetic pathways may cause aberrant human brain development under hypoxic conditions.

The nervous system is sensitive to a variety of environmental insults, which often occur during critical periods of development. Preterm neonates with a very low birth weight are a high-risk population for brain damage as a result of impaired oxygen delivery¹. Hypoxic conditions around birth can also have detrimental effects on rodent and human brain development and function^{2–4}. However, the precise cellular and molecular events that underlie these pathologies are poorly understood.

In all systems studied to date, cellular and systemic responses to hypoxia are coordinated by the phylogenetically conserved HIF-1 protein, a bHLH-PAS domain-containing transcription factor⁵. HIF-1 transcriptionally regulates a wide variety of target genes to facilitate an increase in anaerobic metabolism in hypoxic cells and to enhance vascularization of hypoxic tissues^{6–9}. In normal (normoxic) conditions, HIF-1 protein is efficiently degraded by a conserved proteasomal degradation pathway (Fig. 1a)¹⁰. Degradation is initiated by hydroxylation of a specific proline residue in the conserved LXXLAP motif of HIF-1 by the oxygen-dependent prolyl 4-hydroxylase EGL-9 (ref. 11). The E3 ubiquitin ligase VHL-1 (von Hippel-Lindau tumor suppressor protein) recognizes the hydroxylated proline and targets HIF-1 for ubiquitin-mediated proteasomal degradation¹¹. Hypoxic conditions inhibit the hydroxylation of HIF-1, thereby stabilizing the protein and allowing it to transcriptionally regulate the expression of a host of target genes involved in promoting the survival of animals under hypoxia^{8,9}.

As the precise cellular and molecular events that underlie brain pathologies under hypoxic conditions are poorly understood, we used the nematode *C. elegans* to elucidate the effects of hypoxic exposure on the development of the nervous system. We found that hypoxia induced highly specific neurodevelopmental defects that

are caused by the HIF-1-dependent misregulation of a specific axon guidance system.

RESULTS

Hypoxia causes specific neurodevelopmental defects

We analyzed the development of a number of individual neuronal cell types in *C. elegans* under normoxic (21% oxygen) and hypoxic (1% oxygen) conditions using *gfp* reporter technology. We found that the axons of several motor- and interneuron classes aberrantly crossed the ventral midline under hypoxic conditions during embryonic and larval development (PVQ, PVP and HSN; Fig. 1b–h and Supplementary Table 1 online). The migratory path of the HSN motor neurons was also disrupted (Fig. 1g,i). Moreover, the circumferential trajectory of embryonic motor axons was affected (Fig. 1j,k). The defects that we observed were markedly specific for neuron type, as the axonal development of other ventral cord interneuron classes (AVK and PVT) or the migratory path of other neurons (CAN cells and touch receptor neurons) were unaffected by hypoxia (Supplementary Table 1).

To test whether the neuronal defects that we observed under hypoxic conditions are controlled by *hif-1*, we examined axon pathfinding of the PVQ interneurons in hypoxic conditions in the absence of *hif-1*, using a strain carrying a *hif-1* null mutation, *ia04* (ref. 12). We found that the hypoxia-induced PVQ axon-pathfinding defects were efficiently suppressed by the loss of *hif-1* (Fig. 1c), indicating that hypoxia induces neuronal defects by stabilizing HIF-1 protein and concomitant induction or repression of HIF-1 target genes. To assess whether the effect of HIF-1 on axon pathfinding is controlled by components of its previously described post-translational regulatory machinery, we used a null allele of the *vhl-1* gene that had previously not been molecularly

Department of Biochemistry and Molecular Biophysics, Howard Hughes Medical Institute, Columbia University Medical Center, New York, New York 10032, USA. Correspondence should be addressed to R.P. (rp2184@columbia.edu) or O.H. (or38@columbia.edu).

Received 16 May; accepted 2 June; published online 29 June 2008; doi:10.1038/nn.2152

characterized (*ok161*) (Fig. 2a). *vhl-1(ok161)* null-mutant animals were viable, but showed a highly penetrant PVQ axon-pathfinding defect along the ventral midline that was indistinguishable from the defects that we observed under hypoxic conditions (Fig. 1e,f). Double mutant analysis showed that this defect is fully dependent on *hif-1* (Fig. 2b). Similarly, mutations in *egl-9* (*sa307*, *gk277* and *ok478* alleles) caused qualitatively analogous defects in PVQ axon pathfinding that were *hif-1* dependent (Fig. 2b and data not shown). The weaker penetrance of defects observed in *egl-9* mutants compared with *vhl-1* mutants could result from the fact that none of the available *egl-9* alleles are completely null or that other hydroxylases are involved in regulating HIF-1 stability in this context.

Where does *hif-1* act to affect axon pathfinding and neuronal migration? Both *hif-1* (ref. 12) and *vhl-1* (Fig. 2a) are ubiquitously expressed during embryonic development, thereby yielding no specific clues regarding the sites of gene action. To assess the cellular focus of *hif-1* action, we engineered transgenic strains that express a stabilized version of *hif-1* under the control of cell type-specific promoters. We stabilized HIF-1 by mutating proline 621 in the conserved LXXLAP motif, which is required for degradation of HIF-1 by the *egl-9/vhl-1*-dependent degradation pathway^{10,11}. We mutated the conserved proline to alanine and fused this modified *hif-1* cDNA to a yellow fluorescent protein-encoding cDNA, which allowed us to visualize the increased stability of this mutated protein compared with wild-type protein (Supplementary Table 2 online). To confirm that this 'undegradable'

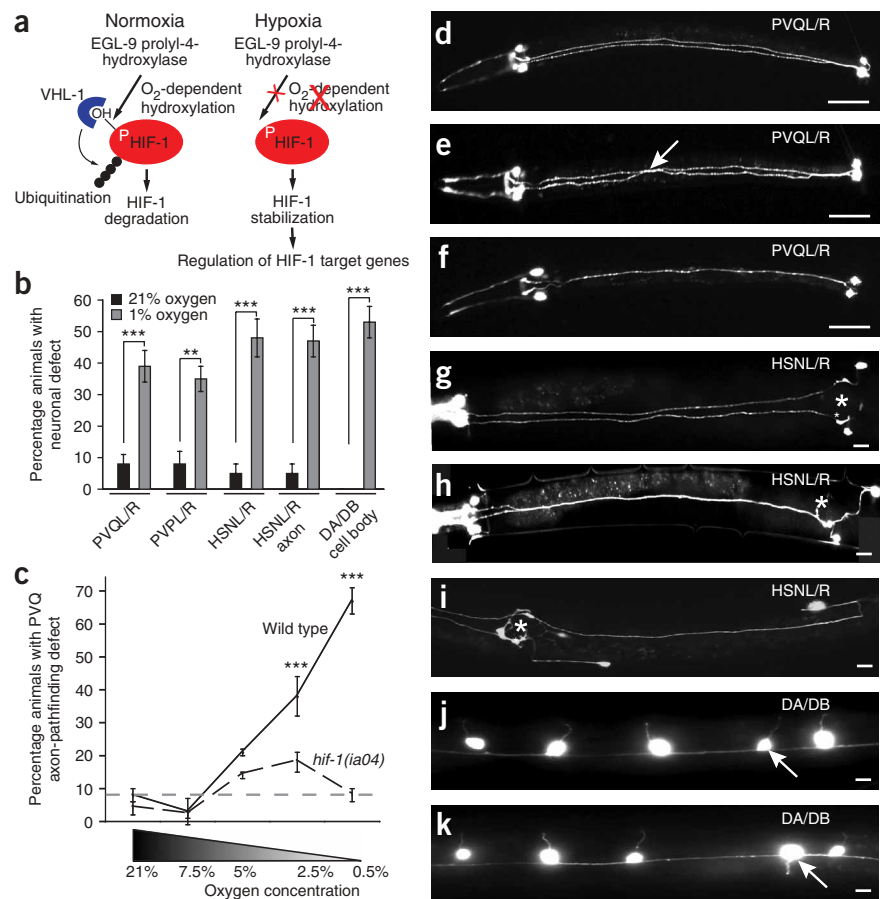
form of HIF-1 (HIF-1^{P621A}) reproduces the effects of hypoxia, we drove HIF-1^{P621A} expression under the control of its own ubiquitously expressed promoter. We found that such expression reproduced the HSN cell migration and PVQ and HSN axon-pathfinding defects that are induced by hypoxic conditions (Fig. 2c). We then expressed HIF-1^{P621A} under the control of three different heterologous promoters in neuronal (*unc-14*), muscle (*unc-120*) or hypodermal/skin (*dpy-7*) cells. Pan-neuronal HIF-1^{P621A} expression produced the same defects as we observed when using the ubiquitous *hif-1* promoter (Fig. 2c). HIF-1^{P621A} driven in muscle also caused defects in PVQ and HSN axon pathfinding, but not in HSN cell migration (Fig. 2c). Hypodermal expression of HIF-1^{P621A} did not affect axon guidance or cell migration (Fig. 2c). To further narrow the cellular focus of HIF-1 action in the nervous system, we assayed HSN axon outgrowth in transgenic animals expressing HIF-1^{P621A} in either the HSN cells themselves or the midline motor neurons, the cells that define the embryonic midline in *C. elegans*¹³. We found that HIF-1 acted non-autonomously in midline neurons to affect outgrowth of the HSN axon along the ventral midline (Fig. 2c). We conclude that stabilized HIF-1 can cause specific neuronal defects in a non-cell autonomous fashion.

daf-2-regulated ROS levels affect axon guidance

Vertebrate HIF-1 protein is also stabilized by unknown means via a burst of reactive oxygen species (ROS) produced by mitochondria under hypoxic conditions (Fig. 3a)^{14,15}. To test whether increased ROS

Figure 1 Hypoxia causes cell-specific defects in the *C. elegans* nervous system. (a) Schematic of the conserved HIF-1 degradation pathway^{10,11}.

(b) Development in 1% O₂ caused axon-pathfinding defects in PVQL/R and PVPL/R interneurons, axon-pathfinding and cell-migration defects in HSNL/R motor neurons, and left/right choice defects in DA/DB motor neurons (*n* = 96–238). Black bars, normoxia; gray bars, 1% O₂. Data were combined from three independent experiments. Statistical significance was assessed by comparing each strain reared under normoxic or hypoxic conditions (z test; ***P* < 0.01, ****P* < 0.005). (c) Penetrance of PVQL/R defects in axon pathfinding increased with decreasing O₂ levels in wild-type worms (*n* = 123–238, black line). Hypoxic conditions interfered with axon pathfinding only during embryogenesis, when PVQL/R axon outgrowth occurs, but not during postembryonic development (data not shown). PVQL/R development was unaffected by hypoxia in *hif-1(ia04)* worms (*n* = 97–133, black dashed line). Gray dashed line represents the background level of PVQ defects under normoxic conditions. Hypoxic wild-type worms were compared with hypoxic *hif-1* mutant and normoxic wild-type animals (z test; ****P* < 0.005). Data were combined from three independent experiments. (d–f) PVQL/R axonal development in normoxia (d) and 1% O₂ (e,f). During hypoxia, the PVQR axon crossed the midline into the left fascicle (arrow, e) or PVQL followed PVQR along its entire length in the right fascicle (f). (g–i) HSNL/R development in normoxia (g) and 1% O₂ (h,i). During normoxia, HSN cell bodies migrate to the vulva and extend axons in the left and right fascicles of the ventral nerve cord (g). During hypoxia, HSNL/R showed axon-pathfinding and cell body migration defects (h,i). Vulval position marked with an asterisk. (j,k) DA/DB commissural development in normoxia (j) and 1% O₂ (k). Arrows point to the DB5 motor neuron that extended a commissure on the left side in normoxia and on the right side in this hypoxic worm. Ventral views, posterior to the right. Scale bars represent 20 μm.



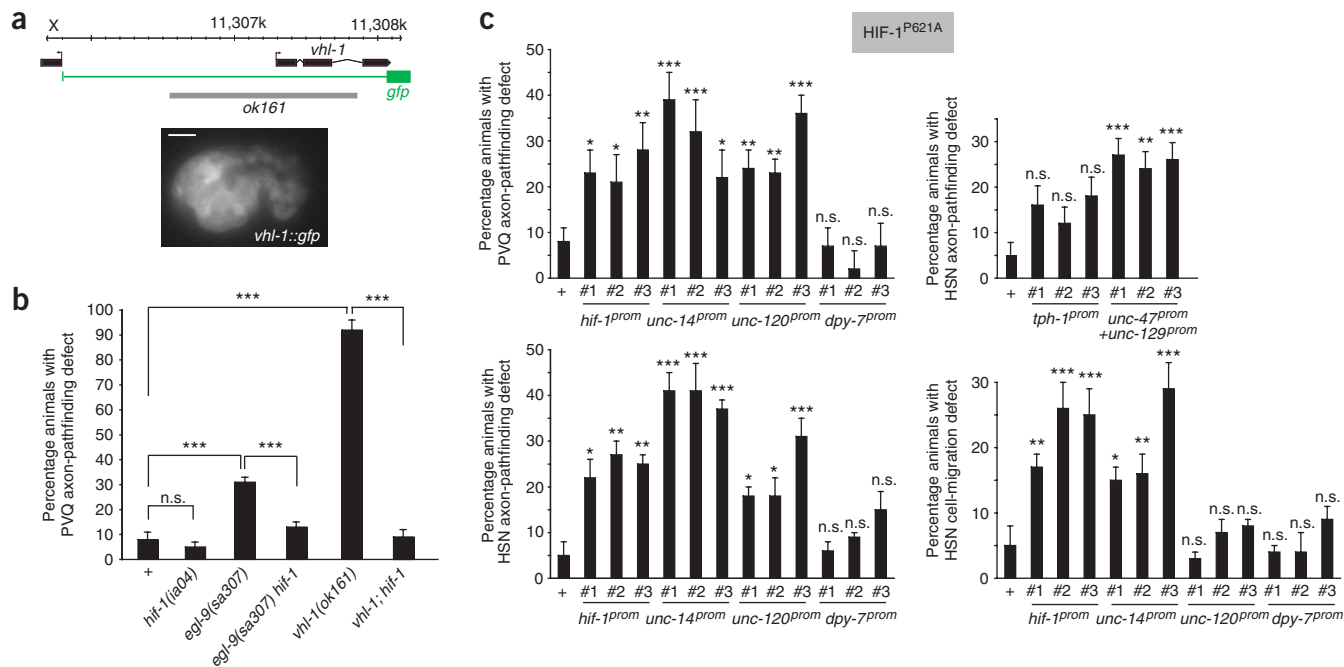


Figure 2 The conserved HIF-1 regulatory pathway mediates the effects of hypoxia on nervous system development. (a) Structure of the previously undescribed *vhl-1(ok161)* deletion allele, a probable null allele (gray bar represents the *ok161* deletion). The region used to drive GFP expression is shown in green. We observed broad expression of this translational *vhl-1::gfp* fusion throughout a developing embryo at the comma stage. Scale bar represents 10 μ m. (b) Mutations of components in the HIF-1 regulatory machinery caused PVQL/R axon-pathfinding defects (midline crossover defects similar to those shown in Fig. 1e,f; $n \geq 90$). The defects observed with the *ok161* allele were confirmed by RNAi directed against *vhl-1* (data not shown). The *egl-9* mutant defects were also observed using two additional *egl-9* alleles, *gk277* and *ok478* (data not shown). Error bars indicate the standard error of proportion and statistical significance was assessed by the z test (** $P < 0.005$, n.s. = not significantly different from control). (c) Neuronal defects caused by expression of a HIF-1^{P621A} cDNA under the control of various different promoters, as indicated (*unc-14^{prom}*, pan-neuronal; *unc-120^{prom}*, muscle; *dpy-7^{prom}*, hypodermal; *tph-1^{prom}*, HSN specific; *unc-47^{prom}* + *unc-129^{prom}*, motor neuron specific; $n = 34$ –238; # refers to independent lines examined for a given transgene). Error bars indicate standard error of the proportion. Statistical significance was assessed by comparing each transgenic line with control animals (z test, * $P < 0.05$, ** $P < 0.01$, *** $P < 0.005$, n.s. = not significantly different from control).

levels in otherwise normoxic conditions can cause axon-pathfinding defects, we analyzed the effect of compromising the activity of antioxidant enzymes that normally degrade ROS. We reduced or eliminated the activity of three superoxide dismutases and two catalases with null mutant alleles provided by the *C. elegans* knockout consortia and RNA interference (RNAi; Fig. 3b,c). We found that null mutations in the superoxide dismutase genes *sod-1* and *sod-4* caused PVQ axon-pathfinding defects that were similar to those observed under hypoxic conditions (Fig. 3c). Disruption of catalase function using a null mutation in *ctl-2* or RNAi against *ctl-1* caused similar defects (Fig. 3c). The defects were most prominent in animals lacking *sod-1*, a Cu²⁺/Zn²⁺ superoxide dismutase that functions in the cytoplasm, the site of HIF-1 hydroxylation¹⁶. The axonal defects of *sod-1* mutants were significantly suppressed in *sod-1; hif-1* double mutants ($P < 0.05$; Fig. 3c), demonstrating that ROS act through *hif-1* to affect axon pathfinding. A *sod-1* transcriptional GFP fusion (*sod-1^{prom}::GFP*) was expressed in multiple tissues in the embryo (Supplementary Fig. 1 online), and we found that transgenic expression of *sod-1* under the control of pan-neuronal or muscle promoters rescued the PVQ defects of *sod-1(tm776)* mutant animals, demonstrating both a cell-autonomous and a non-cell autonomous focus of action for *sod-1* (Fig. 3c). Consistent with this, overexpression of *sod-1* in the nervous system or muscle of wild-type animals also rescued the axonal defects that we observed in hypoxic conditions (Fig. 3d and Supplementary Fig. 1). Together with the defects that were observed on either neuronal or muscle expression of undegradable HIF-1, these data suggest that

ROS accumulation in either of these tissues leads to HIF-1 stabilization and subsequent PVQ axon-pathfinding defects.

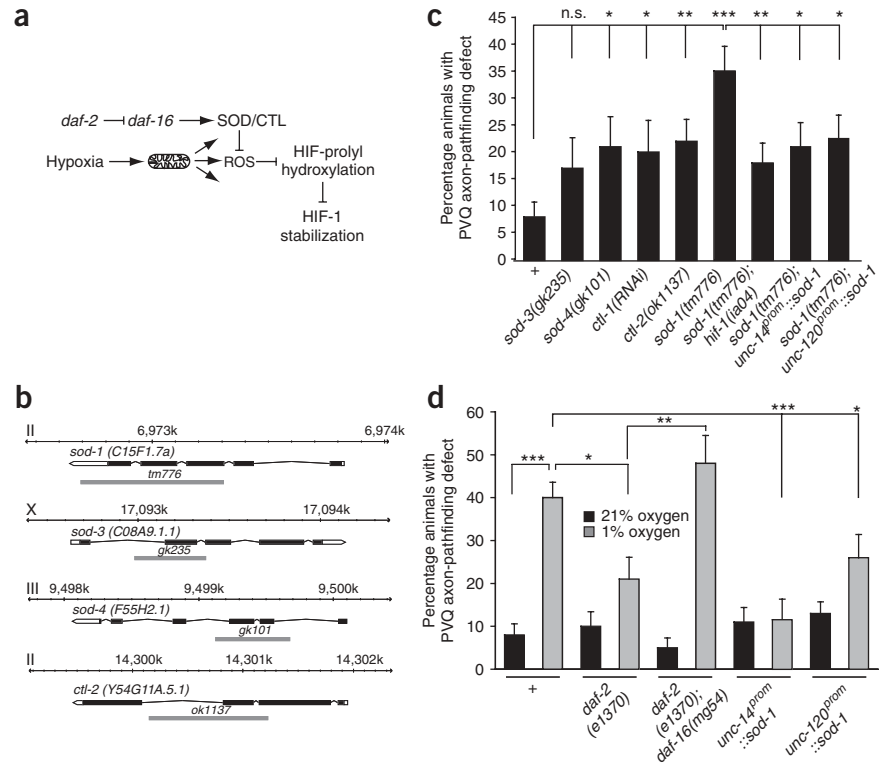
Loss of the *daf-2* insulin/insulin-like growth factor receptor leads to an upregulation in the activity of the *daf-16* FOXO transcription factor, which results in an increased level of expression of antioxidant enzymes such as superoxide dismutases and catalases (Fig. 3a)^{17–20}. As these enzymes dampen ROS levels, their *daf-16*-dependent upregulation in *daf-2* mutants would be predicted to increase HIF-1 degradation in hypoxia. This may in turn diminish the detrimental effects of stabilized HIF-1 protein on axon pathfinding under hypoxic conditions (Fig. 3a). We indeed found that elimination of insulin-like signaling in *daf-2* null mutants suppressed hypoxia-induced axon-pathfinding defects (Fig. 3d). This suppression was reversed by a mutation in *daf-16*, the downstream effector of *daf-2* signaling (Fig. 3d). Loss of *daf-2* did not suppress the axonal defects induced by expression of stabilized HIF-1 (wild-type, 53% \pm 2.6%; *daf-2*, 47% \pm 4.6%; the difference was not statistically significant, $P = 0.3$), indicating that *daf-2* acts upstream of *hif-1*. Taken together, our data suggest that insulin-like signaling permits the accumulation of ROS under hypoxic conditions, thereby stabilizing HIF-1 and causing neurodevelopmental defects. *daf-2* is also involved in suppressing hypoxia-induced cell death²¹, but the involvement of *hif-1* and ROS in this process has not yet been explored.

Aberrant Eph signaling causes hypoxia-induced neuronal defects

We sought to identify target genes through which HIF-1 (and therefore hypoxia and ROS) affects axon pathfinding using a candidate gene

Figure 3 Reduction of *daf-2* signaling suppresses hypoxia-induced PVQ/R axon-pathfinding defects, probably through detoxification of ROS.

(a) Schematic showing that hypoxia induces a surge of ROS from mitochondria^{14,15} resulting in HIF-1 stabilization. *daf-2* signaling controls superoxide dismutase and catalase levels via DAF-16 (refs. 19,20). (b) Structures of detoxifying enzyme deletion alleles used. On the basis of the domains eliminated, all alleles are probably molecular nulls. Gray bars represent the deletions. (c) Reduction of antioxidant enzyme function in normoxia caused PVQ axon-pathfinding defects (midline crossover defects similar to those shown in Fig. 1e,f). The strongest defects were observed in *sod-1(tm776)* mutants. These defects were suppressed in *sod-1(tm776); hif-1(ia04)* double mutants and rescued with *sod-1* overexpression in the nervous system or in muscle (*unc-14* and *unc-120* promoters respectively, $n = 46$ –238). Error bars indicate the standard error of proportion and statistical significance was assessed by the z test ($*P < 0.05$, $**P < 0.01$, $***P < 0.005$, n.s. = not significantly different from control). (d) Suppression of hypoxia-induced PVQ axon-pathfinding defects in the *daf-2(e1370)* mutant was fully rescued in the *daf-2(e1370); daf-16(mg54)* double mutant. Moreover, *sod-1* overexpression in the nervous system or muscle (*unc-14* and *unc-120* promoters, respectively) rescued the hypoxia-induced PVQ pathfinding defects ($n = 189$ –238). Data for other rescuing lines are in **Supplementary Figure 1**. Black bar, normoxia; gray bars, 1% O₂. Statistical significance was assessed by comparing with normoxic control or single mutant where applicable (z test). Data were combined from three independent experiments.



approach. Microarray analysis has revealed scores of genes that appear to be controlled by *hif-1* (refs. 8,9). Both datasets^{8,9} indicate that the Eph receptor tyrosine kinase *vab-1*, which was previously implicated in controlling axon pathfinding in the ventral nerve cord of *C. elegans*¹³ and cell migration in the embryo²², is upregulated. Using semiquantitative RT-PCR, we confirmed that *vab-1* mRNA levels were indeed upregulated in hypoxic wild-type nematodes and in HIF-1-stabilized *vhl-1* mutants (Fig. 4a). As expected, this upregulation was abolished in *hif-1* mutants (Fig. 4a). We asked whether increased ephrin receptor signaling was responsible for the PVQ pathfinding defects that we observed in hypoxic animals. We found that the hypoxia-induced PVQ defects were significantly suppressed in *vab-1* mutant animals ($P < 0.05$; Fig. 4b). Similarly, the *vhl-1*- and HIF-1^{P621A}-induced PVQ defects were also suppressed in *vab-1* mutant backgrounds (Fig. 4c,d).

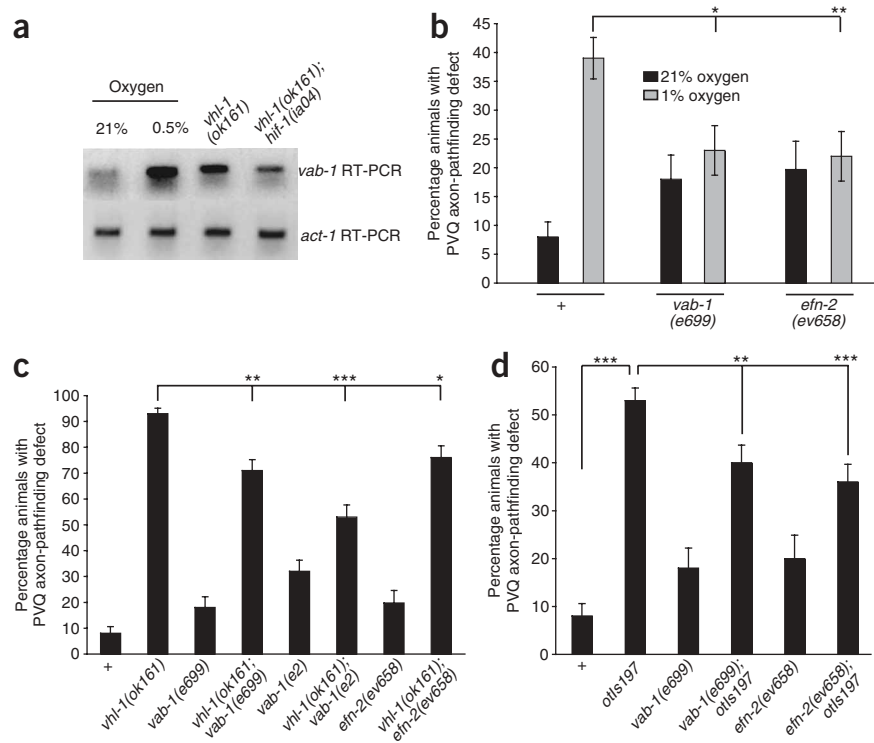
Our genetic epistasis analysis demonstrates that the hypoxia- and *hif-1*-induced upregulation of *vab-1* is required, at least in part, to induce axon-pathfinding defects. However, are increases in *vab-1* expression also sufficient to cause such defects? To test this possibility, we generated transgenic animals that express *vab-1* under the control of heterologous promoters in an otherwise wild-type background (Fig. 5). Multiple independent transgenic lines in which *vab-1* was expressed under a pan-neuronal promoter showed axon-pathfinding defects, indicating the sufficiency of *vab-1* in the nervous system for aberrantly affecting axonal development at the midline under hypoxic conditions (Fig. 5a). The *vab-1*-overexpression effect on axonal development was suppressed by removal of *efn-2* (Fig. 5d), indicating that the correct balance of Eph receptor signaling at the midline is important and rendering it unlikely that *vab-1* overexpression nonspecifically interferes with other signaling pathways.

To further narrow the neuronal focus of action for overexpressed *vab-1*, we used HSN axon pathfinding as a model. The axonal growth cone of the HSN neuron migrates along the ventral midline, which is defined by midline motor neurons¹³. To determine whether *vab-1* acts autonomously in HSN to affect axon growth along the midline or whether it acts non-autonomously in the midline motor neurons, we overexpressed *vab-1* in the respective neuron types. We found that overexpression in midline motor neurons and not in the HSN neurons caused HSN axon-pathfinding defects (Fig. 5b). These results match the non-autonomous mode of action that we found when HIF-1^{P621A} was overexpressed in midline motor neurons, but not in HSN neurons (Fig. 2c). We conclude that hypoxia/HIF-1-mediated upregulation of *vab-1* in the nervous system non-autonomously disrupts axon patterning at the ventral midline.

In contrast with ectopic neuronal expression, ectopic muscle expression of *vab-1* did not cause axonal defects (Fig. 5a). Consistent with this result, the axonal defects that we observed on muscle expression from stabilized HIF-1 may be caused by dysregulation of a gene other than *vab-1*. This gene probably acts in the ephrin receptor pathway, as hypoxia-induced (and therefore HIF-1 induced) axonal defects were suppressed by removal of *vab-1*. One possibility would be that muscle-expressed, stabilized HIF-1 may cause upregulation of an ephrin ligand, which may repel axons away from muscle across the midline. We tested this possibility by generating transgenic lines overexpressing the ephrin *efn-2* in muscle. These worms showed axon midline crossover defects (neuronal overexpression of *efn-2* did not cause such axonal defects; Fig. 5c). If upregulation of *efn-2* were indeed important in hypoxia-induced axon midline defects, the defects induced by hypoxia, as well as those induced by *vhl-1* and neuronally expressed HIF-1^{P621A} should be at least partly alleviated by genetic removal of *efn-2*. We found this to

Figure 4 *vab-1* is upregulated by hypoxia and causes PVQL/R axon-pathfinding defects.

(a) Semicquantitative RT-PCR of *vab-1* and *act-1* (control) mRNA levels. *vab-1* message was upregulated in wild-type worms grown in 0.5% O₂ compared with normoxic animals. Upregulation of *vab-1* in the *vhf-1(ok161)* mutant was suppressed in the *vhf-1(ok161); hif-1(ia04)* double mutant. We used 1 μg of total RNA from a mixed stage population as a template. RT-PCR analysis was triplicated on two independently extracted total RNA samples for each condition and one representative example is shown. (b) *vab-1(e699)* and *efn-2(ev658)* mutations suppressed the hypoxia-induced PVQ axon-pathfinding defects ($n = 97$ –238). Data were combined from three independent experiments. Black bars, normoxia; gray bars, 1% O₂. Statistical significance was assessed by comparing each strain reared under normoxic or hypoxic conditions (z test, $*P < 0.05$, $**P < 0.01$). (c) *vab-1* hypomorphic mutations in the ephrin-binding domain (*e699*) and the tyrosine kinase domain (*e2*) and a mutation in *efn-2(ev658)* suppressed the PVQ axon-pathfinding defects observed in *vhf-1(ok161)* worms ($n = 58$ –238). Statistical significance was assessed by comparing single and double mutant combinations (z test, $*P < 0.05$, $**P < 0.01$, $***P < 0.005$). (d) Artificially stabilized HIF-1 (HIF-1^{P621A}) expressed under a pan-neuronal promoter (*otIs197*) caused defects in PVQ axon pathfinding. These pathfinding defects were significantly suppressed by mutations in downstream factors, *vab-1(e699)* and *efn-2(ev658)* ($n = 66$ –370). Error bars represent standard error of the proportion. Statistical significance was assessed by comparing with *otIs197* alone (z test, $**P < 0.01$, $***P < 0.005$).



be the case (Fig. 4b–d). Taken together, these results indicate that dysregulation of Eph receptor signaling is a critical component of hypoxia-induced axonal misrouting (Supplementary Fig. 2 online).

It would seem paradoxical that HIF-1, which is known to have a protective effect against hypoxia, upregulates a gene whose only role is to cause neurodevelopmental defects such as those attributed to the upregulation of *vab-1*. A possible explanation for this is that *vab-1* has another function during hypoxia. Indeed, the viability of *vab-1* null mutant animals is significantly impaired under hypoxic conditions ($P < 0.005$; Fig. 5e). Kinase-defective *vab-1* mutants (*e2* allele) showed similar defects (data not shown), indicating that VAB-1 kinase activity is necessary for protection during hypoxia. Enhanced embryonic lethality is probably the result of inappropriate cell migrations in the gastrulating embryo, as we observed severe defects in hypodermal morphogenesis of *vab-1(dx31)* embryos grown in hypoxia (Fig. 5e). From these observations, we conclude that *vab-1* and its *hif-1*-dependent upregulation under hypoxic conditions are required to promote viability in wild-type animals.

DISCUSSION

Our results demonstrate that oxygen levels cause cell-specific defects in the *C. elegans* nervous system by stabilizing HIF-1 in neurons and muscle. Neuronal and muscle ROS levels also affect nervous system development via the stabilization of HIF-1. Through the regulation of ROS levels, insulin-like receptor signaling also affects HIF-1 stability and axon pathfinding, thereby extending the known functions of this signaling pathway in controlling metabolism and life span to a previously non-appreciated role in nervous system development.

Hypoxia and ROS-mediated stabilization of HIF-1 causes nervous system defects, at least partially, by upregulating VAB-1. The

consequences of upregulating VAB-1 or VAB-1 loss¹³ are essentially the same; axons failed to be guided along the ventral midline, defined by embryonic motor neurons (Supplementary Fig. 2). In the case of a loss of VAB-1, this effect is caused by the loss of a cell-autonomous role of VAB-1 in the growth cone of the axons guided along midline motor neurons, which provide a repulsive barrier through ephrin expression¹³ (Supplementary Fig. 2). In contrast, the axonal midline defects that we observed on HIF-1-induced upregulation of VAB-1 in hypoxic conditions resulted from a non-autonomous function of EFN-2-activated VAB-1 in midline motor neurons, which apparently disrupts the guidepost function of midline motor neurons, thereby allowing aberrant axon midline crossover (Supplementary Fig. 2).

How could aberrant VAB-1 signaling have such an effect on midline neurons? Studies in vertebrates have shown that Eph receptor signaling can interact with other receptor tyrosine kinase signaling pathways, such as the fibroblast growth factor receptor (FGFR)/Ras signaling pathway or the Wnt-dependent Ryk pathway²³. We found that both the FGFR/Ras signaling pathway²⁴ and the Ryk/*lin-18* receptor tyrosine kinase (T. Boulin at Columbia University, now École Normale Supérieure, and O.H., unpublished data) are also required for midline axon pathfinding in *C. elegans*. It is conceivable that hypoxia-induced VAB-1 overexpression in midline neurons may interfere with these pathways. For example, in the context of FGFR signaling, either reducing or overactivating *let-60/ras* signaling with a *let-60/ras* gain-of-function allele causes axon midline guidance defects²⁴. In vertebrates, Eph receptor can, depending on the cellular context, activate or attenuate Ras signaling²³. Analogously, VAB-1 overexpression may also inappropriately interfere with *let-60/ras* signaling at the ventral midline, thereby causing the defects that we observed. In

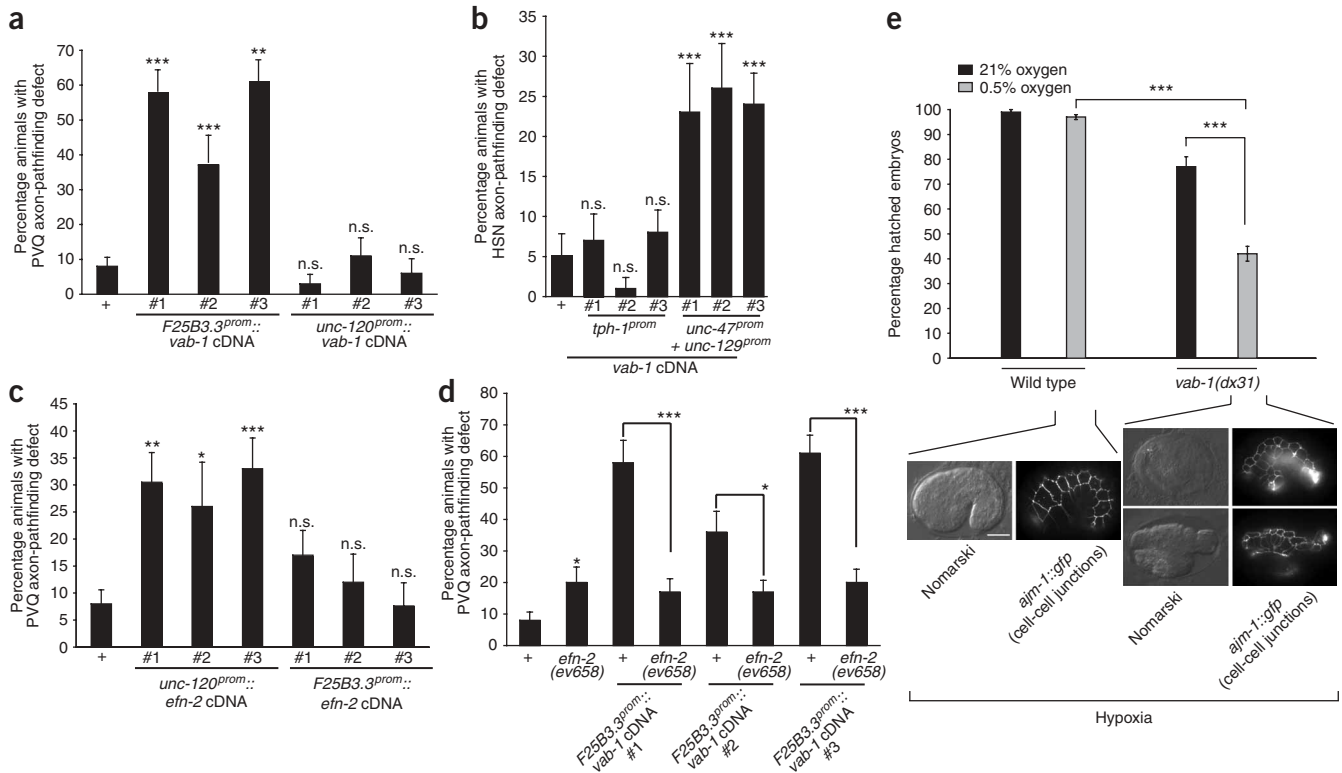


Figure 5 *vab-1* acts non-autonomously to cause axon-pathfinding defects. **(a)** Overexpression of *vab-1* cDNA under control of the pan-neuronal *F25B3.3* promoter, but not the muscle *unc-120* promoter, caused PVQ axon-pathfinding defects ($n = 42$ – 238). A control cDNA (*dsRed2*), driven by the *F25B3.3* promoter, caused no PVQ defects (data not shown). **(b)** Overexpression of *vab-1* cDNA under the control of the embryonic midline motor neuron drivers *unc-47* (DD neurons) and *unc-129* (DA, DB neurons), but not under the control of the HSN-driver *tph-1*, caused HSN axon-pathfinding defects ($n = 53$ – 139). **(c)** Overexpression of *efn-2* cDNA under the control of the muscle *unc-120* promoter, but not the pan-neuronal *unc-14* promoter, caused PVQ axon-pathfinding defects ($n = 31$ – 238). # indicates independent transgenic lines. Statistical significance was assessed by comparing transgenic with nontransgenic controls (z test, * $P < 0.05$, ** $P < 0.01$, *** $P < 0.005$, n.s. = not significantly different from controls). **(d)** The PVQ pathfinding defects caused by overexpression of *vab-1* in the nervous system resulted from disruption of ephrin signaling and not of another unrelated signaling pathway. Loss of the ephrin ligand, *efn-2*, significantly suppressed the defects caused by pan-neuronally expressed *vab-1* ($n = 48$ – 104). Error bars represent standard error of the proportion. Statistical significance was assessed by comparing each transgenic line with and without *efn-2^{ev658}* (z test). **(e)** Exposure of *vab-1(dx31)* null mutant embryos to 0.5% O_2 significantly increased embryonic lethality when compared with wild type. Eight broods were scored ($n \geq 750$). Black bars, normoxia; gray bars, 0.5% O_2 . Micrographs of embryos below the graphs show Nomarski images (left) and fluorescent images (right) in which hypodermal cells are visualized with the *ajm-1::GFP* adherens junction marker (strain *jcls1*). Hypoxic wild-type animals are shown to the left and hypoxic *vab-1(dx31)* embryos to the right. Scale bar represents 10 μm .

in addition to these possibilities, it should be kept in mind that a plethora of other pathways have been implicated in axon midline patterning in worms, including integrin, semaphorin and netrin signaling²⁵. Each of these signaling systems could potentially be sensitive to hypoxia-induced overexpression of VAB-1. Whatever the precise mechanism, our results indicate that the detrimental effect of *vab-1* upregulation seems to be the price to pay for the protective role *vab-1* has during hypoxic embryonic development, in which *vab-1* is known to be required for neural and epithelial morphogenesis during gastrulation²².

The cellular and molecular consequences of hypoxia that we describe here may be conserved, as HIF-1-dependent upregulation of ephrin signaling components also occurs in mouse ectodermal tissue²⁶. Moreover, hypoxia can affect axon outgrowth of a rat neuronal cell line²⁷. Although neuronal loss has been recognized as a consequence of hypoxic conditions during human brain development^{2,3}, our demonstration of cell type-specific axon-pathfinding and cell-migration defects under hypoxic conditions suggest that the defects in human brain function observed after hypoxic insults may be caused by a whole

spectrum of distinct developmental defects that are controlled by highly conserved signaling pathways.

METHODS

Strains and reporter transgenes. We used the following worm strains: N2 Bristol (wild type), *daf-16(mg54)*, *ctl-1(ok1137)*, *sod-1(tm776)*, *vab-1(e2, e699 and dx31)*, *daf-2(e1370)*, *efn-2(ev658)*, *sod-4(gk101)*, *egl-9(sa307, gk277 and ok478)*, *hif-1(ia04)*, *sod-3(gk235)*, *vhl-1(ok161)*. Alleles are presented in parentheses.

The reporter transgenes that we used were *oys14 Is[sra-6::GFP]* for PVQ neurons, *hdl26 Is[sra-6::DsRed2]*; *odr-1::GFP* for PVP neurons, *zdl13 Is[tph-1::GFP]* for HSN neurons, *ev1s82b Is[unc-129::GFP]* for DA/DB neurons, *bw1s2 Is[flp-1::GFP]* for AVK neurons, *ot1s39 Is[unc-47 delta::GFP]* for PVT neurons, *zdl5 Is[mec-4::GFP]* for touch cells, *ot1s33 Is[kal-1::GFP]* for CAN cells and *jcls1 Is[ajm-1::GFP]* for hypodermal cells. Wormbase designations are given for each transgene. See **Supplementary Methods** online for additional arrays used in this study.

DNA construction and injection. A list of all constructs and primers used can be found in the **Supplementary Methods**. DNA was injected at 5–50 $\mu g \mu l^{-1}$

depending on the experiment, and *ttx-3::rfp* (70 ng μl^{-1}) and *pRF4* (50 ng μl^{-1}) were used as injection markers.

Hypoxic incubation. All animals were maintained at 20 °C. Continuously well-fed young adult hermaphrodites were placed in a hypoxic chamber (C-174 chamber, Biospherix) for 36 h at 25 °C and their progeny were scored. The oxygen concentration was continuously monitored with an oxygen sensor (Pro:Ox oxygen controller, Biospherix) and automatically adjusted with compressed nitrogen.

Scoring of phenotype. Neuronal phenotypes were scored in adult animals using an Axioplan 2 fluorescent microscope.

Semiquantitative RT-PCR analysis. Total RNA was extracted from mixed stage populations with Trizol (Invitrogen) and was then treated with DnaseI (Fermentas). RT-PCR amplification of *vab-1* and *act-1* (control) mRNA was carried out on 1 μg of these total RNA samples using Superscript One-Step RT-PCR with Platinum Taq (Invitrogen). We used gene-specific oligos that were designed to anneal to either side of an intron to distinguish between DNA and RNA amplification. For *vab-1*, our forward primer was 5'-ATC AGA GAG CCT ACG TCA CG-3' and our reverse primer was 5'-CGT CAT ATT TGA ATT ACT TCG AGC-3'. For *act-1*, our forward primer was 5'-CTT GGG TAT GGA GTC CGC C-3' and our reverse primer was 5'-TTA GAA GCA CTT GCG GTG AAC-3'.

RNAi. RNAi was carried out as described previously²⁸. Several individual hermaphrodites were plated at the L3 or L4 stage onto NGM agar plates (with 6 mM IPTG and 100 $\mu\text{g ml}^{-1}$ ampicillin) that had been seeded with bacteria expressing dsRNA and were maintained on the plates for 48 h at 15 °C. Single adults were then transferred onto freshly seeded plates at 20 °C and their progeny were analyzed for neuroanatomical defects.

Note: Supplementary information is available on the Nature Neuroscience website.

ACKNOWLEDGMENTS

We thank Q. Chen for expert technical assistance in generating transgenic strains, A. Clarke for technical help, the *Caenorhabditis* Genetics Center and J.A. Powell-Coffman for providing strains, M. Krause for the *unc-120* promoter, the *C. elegans* knockout consortia lead by R. Barstead, D. Moerman and S. Mitani for *gk*, *ok* and *tm* alleles, respectively, T. Boulin for the *pF25B3.3::vab-1* construct and communicating results on *lin-18*, and I. Greenwald and members of the Hobert lab for comments on the manuscript. This work was funded in part by the Muscle Dystrophy Association (O.H.). O.H. is an investigator of the Howard Hughes Medical Institute.

AUTHOR CONTRIBUTIONS

R.P. designed and conducted the experiments and wrote the manuscript. O.H. supervised the project, gave suggestions and helped write the manuscript.

Published online at <http://www.nature.com/natureneuroscience/>

Reprints and permissions information is available online at <http://npg.nature.com/reprintsandpermissions/>

1. Arpino, C. *et al.* Brain damage in preterm infants: etiological pathways. *Ann. Ist. Super. Sanita* **41**, 229–237 (2005).

2. Inder, T.E. & Volpe, J.J. Mechanisms of perinatal brain injury. *Semin. Neonatol.* **5**, 3–16 (2000).
3. Berger, R. & Garnier, Y. Pathophysiology of perinatal brain damage. *Brain Res. Brain Res. Rev.* **30**, 107–134 (1999).
4. El-Khodori, B.F. & Boksa, P. Transient birth hypoxia increases behavioral responses to repeated stress in the adult rat. *Behav. Brain Res.* **107**, 171–175 (2000).
5. Semenza, G.L. Hypoxia-inducible factor 1: oxygen homeostasis and disease pathophysiology. *Trends Mol. Med.* **7**, 345–350 (2001).
6. Ratcliffe, P.J., Pugh, C.W. & Maxwell, P.H. Targeting tumors through the HIF system. *Nat. Med.* **6**, 1315–1316 (2000).
7. Iyer, N.V. *et al.* Cellular and developmental control of O₂ homeostasis by hypoxia-inducible factor 1 alpha. *Genes Dev.* **12**, 149–162 (1998).
8. Shen, C., Nettleton, D., Jiang, M., Kim, S.K. & Powell-Coffman, J.A. Roles of the HIF-1 hypoxia-inducible factor during hypoxia response in *Caenorhabditis elegans*. *J. Biol. Chem.* **280**, 20580–20588 (2005).
9. Bishop, T. *et al.* Genetic analysis of pathways regulated by the von Hippel-Lindau tumor suppressor in *Caenorhabditis elegans*. *PLoS Biol.* **2**, e289 (2004).
10. Shen, C. & Powell-Coffman, J.A. Genetic analysis of hypoxia signaling and response in *C. elegans*. *Ann. NY Acad. Sci.* **995**, 191–199 (2003).
11. Epstein, A.C. *et al.* *C. elegans* EGL-9 and mammalian homologs define a family of dioxygenases that regulate HIF by prolyl hydroxylation. *Cell* **107**, 43–54 (2001).
12. Jiang, H., Guo, R. & Powell-Coffman, J.A. The *Caenorhabditis elegans hif-1* gene encodes a bHLH-PAS protein that is required for adaptation to hypoxia. *Proc. Natl. Acad. Sci. USA* **98**, 7916–7921 (2001).
13. Boulin, T., Pocock, R. & Hobert, O. A novel Eph receptor-interacting IgSF protein provides *C. elegans* motoneurons with midline guidepost function. *Curr. Biol.* **16**, 1871–1883 (2006).
14. Brunelle, J.K. *et al.* Oxygen sensing requires mitochondrial ROS but not oxidative phosphorylation. *Cell Metab.* **1**, 409–414 (2005).
15. Chandel, N.S. *et al.* Mitochondrial reactive oxygen species trigger hypoxia-induced transcription. *Proc. Natl. Acad. Sci. USA* **95**, 11715–11720 (1998).
16. Jensen, L.T. & Culotta, V.C. Activation of CuZn superoxide dismutases from *Caenorhabditis elegans* does not require the copper chaperone CCS. *J. Biol. Chem.* **280**, 41373–41379 (2005).
17. Vanfleteren, J.R. & De Vreese, A. The gerontogenes *age-1* and *daf-2* determine metabolic rate potential in aging *Caenorhabditis elegans*. *FASEB J.* **9**, 1355–1361 (1995).
18. Honda, Y. & Honda, S. The *daf-2* gene network for longevity regulates oxidative stress resistance and Mn-superoxide dismutase gene expression in *Caenorhabditis elegans*. *FASEB J.* **13**, 1385–1393 (1999).
19. Murphy, C.T. *et al.* Genes that act downstream of DAF-16 to influence the lifespan of *Caenorhabditis elegans*. *Nature* **424**, 277–283 (2003).
20. Panowski, S.H., Wolff, S., Aguilaniu, H., Durieux, J. & Dillin, A. PHA-4/Foxa mediates diet-restriction-induced longevity of *C. elegans*. *Nature* **447**, 550–555 (2007).
21. Scott, B.A., Avidan, M.S. & Crowder, C.M. Regulation of hypoxic death in *C. elegans* by the insulin/IGF receptor homolog DAF-2. *Science* **296**, 2388–2391 (2002).
22. George, S.E., Simokat, K., Hardin, J. & Chisholm, A.D. The VAB-1 Eph receptor tyrosine kinase functions in neural and epithelial morphogenesis in *C. elegans*. *Cell* **92**, 633–643 (1998).
23. Murai, K.K. & Pasquale, E.B. 'Eph'ective signaling: forward, reverse and crosstalk. *J. Cell Sci.* **116**, 2823–2832 (2003).
24. Bülow, H.E., Boulin, T. & Hobert, O. Differential functions of the *C. elegans* FGF receptor in axon outgrowth and maintenance of axon position. *Neuron* **42**, 367–374 (2004).
25. Hobert, O. & Bülow, H. Development and maintenance of neuronal architecture at the ventral midline of *C. elegans*. *Curr. Opin. Neurobiol.* **13**, 70–78 (2003).
26. Vihanto, M.M. *et al.* Hypoxia upregulates expression of Eph receptors and ephrins in mouse skin. *FASEB J.* **19**, 1689–1691 (2005).
27. O'Driscoll, C.M. & Gorman, A.M. Hypoxia induces neurite outgrowth in PC12 cells that is mediated through adenosine A2A receptors. *Neuroscience* **131**, 321–329 (2005).
28. Simmer, F. *et al.* Genome-wide RNAi of *C. elegans* using the hypersensitive rrf-3 strain reveals novel gene functions. *PLoS Biol.* **1**, E12 (2003).